# An Independent-Hot-Spot Approach to Multibeam Laser–Plasma Instabilities

R. K. Follett, H. Wen, D. H. Froula, D. Turnbull, and J. P. Palastro

Laboratory for Laser Energetics, University of Rochester

In laser-driven inertial confinement fusion (ICF), a millimeter-scale cryogenic capsule of deuterium–tritium fuel with a thin outer ablator is imploded by either direct laser illumination (direct drive) or focusing the lasers onto the interior walls of a hohlraum to generate an x-ray bath (indirect drive).[1] In both cases, the many high-intensity laser beams overlapping in underdense plasma can drive various laser–plasma instabilities (LPI's) that can severely inhibit implosion performance.[2,3]

Analytic results for instability behavior are typically limited to the case of a single plane-wave laser driving instability in the linear regime. ICF experiments, however, involve multiple overlapping laser beams, each using a phase plate that generates a complex speckle pattern in the plasma,[4] and accurate predictions of instability behavior require a description that accounts for their combined interaction.[5] Analytic theories for instability behavior in a single speckled beam have been developed using the independent-hot-spot model, where a statistical description of the speckle intensity is combined with the single-speckle instability behavior to predict the global instability behavior.[6,7] Multibeam interactions have historically been described using the common-wave model, where wave-vector matching considerations are used to show that overlapping laser beams can couple to a shared daughter wave propagating along the drive-beam axis of symmetry.[8–13] However, recent experiments and simulations of multibeam LPI's have shown that the common-wave description often fails to predict instability behavior. In particular, laser beams that do not satisfy the geometric requirements imposed by the common-wave matching conditions can still contribute to instability growth.[14–16]

Here we develop a multibeam hot-spot model that provides a more-predictive description of LPI behavior than the widely used common-wave approach. The model is extended to include absolute instability in an inhomogeneous plasma and applied to the two-plasmon–decay (TPD) instability. The excellent agreement with multibeam *LPSE* simulations demonstrates its utility and shows that there is an important qualitative difference between 2-D and 3-D single-speckle instability thresholds that is not present in the plane-wave case and results in lower instability thresholds in 2-D. This approach leads to a new understanding of multibeam instability behavior that can be used to make better quantitative predictions for improving the design of experiments and future laser facilities.

Given a collection of $N$ speckles, the absolute instability threshold occurs when the peak speckle intensity is equal to the single-speckle threshold, $I_M = I_{\mathrm{thr,speckle}}$. Introducing the average laser intensity $I_0$ and ensemble averaging over speckle realizations, this can be written as

$$I_{\mathrm{thr}} = \frac{1}{\left\langle I_M / I_0 \right\rangle} I_{\mathrm{thr,\,speckle}}\,, \tag{1}$$

where we have defined the expected average intensity at threshold $I_{\mathrm{thr}} \equiv \langle I_0 \rangle$. Accordingly, evaluation of the expected threshold in the independent-hot-spot model is reduced to the evaluation of $\left\langle I_M / I_0 \right\rangle$ and $I_{\mathrm{thr,speckle}}$. The expected peak speckle intensity can be written in terms of the probability that every speckle intensity is less than $u$:[17]

$$\left\langle I_M / I_0 \right\rangle = \int_0^\infty \left[1 - P\left(I/I_0 < u\right)^N\right] \mathrm{d}u. \tag{2}$$

Reference 18 derives speckle distributions that are valid for high-intensity speckles but behave badly at low intensities. Accordingly, we use exponential distributions at low intensities to generate probability distributions that behave well at all intensities:

$$P\left(I/I_0 > u\right)_{\text{2-D}} = \begin{cases} e^{-u/\mu_2}, & u < u_{\text{s2}} \\ A_2\left[\left(\frac{1}{2}+\frac{\pi}{4}\right)u + \frac{1}{2}\right]e^{-u}, & u > u_{\text{s2}} \end{cases}, \tag{3}$$

$$P\left(I/I_0 > u\right)_{\text{3-D}} = \begin{cases} e^{-u/\mu_3}, & u < u_{\text{s3}} \\ A_3\left[u^{3/2} - \frac{3}{10}u^{1/2}\right]e^{-u}, & u > u_{\text{s3}} \end{cases}, \tag{4}$$

where the $\mu_{\text{i}}$ are parameters and the $A_{\text{i}}$ and $u_{\text{si}}$ are chosen to make the distributions and their first derivatives continuous. Here $\mu_2 = \mu_3 = 4$ was chosen on the basis of comparison to simulations, which gives $A_2 = 1.185$, $u_{\text{s2}} = 0.944$, $A_3 = 1.848$, and $u_{\text{s3}} = 2.210$.

Incorporating Eqs. (3) and (4) into Eq. (2), using the binomial theorem, and integrating gives

$$\left\langle I_M/I_0\right\rangle_{\text{2-D}} = \sum_{a=1}^{N}\binom{N}{a}(-1)^a\left[\frac{\mu_2}{a}\left(e^{-au_{\text{s2}}/\mu_2}-1\right) - A_2^a a^{-1-a} e^{2a/2+\pi}\left(\frac{2+\pi}{4}\right)^a \Gamma\left(1+a, \frac{2a}{2+\pi}+au_{\text{s2}}\right)\right], \tag{5}$$

$$\left\langle I_M/I_0\right\rangle_{\text{3-D}} = \sum_{a=1}^{N}\binom{N}{a}(-1)^a\left[\frac{\mu_3}{a}\left(e^{-au_{\text{s3}}/\mu_3}-1\right) - A_3^a \sum_{k=0}^{a}\binom{a}{k}\left(-\frac{3}{10}\right)^k a^{k-1-3a/2}\Gamma\left(1-k+3a/2, au_{\text{s3}}\right)\right], \tag{6}$$

where $\Gamma(s,x)$ is the incomplete gamma function.

To determine $N$, we restrict our discussion to instabilities that are spatially localized by plasma inhomogeneity such that $N$ is the number of speckles in a cross section of the laser field (i.e., the interaction region is not significantly longer than the speckle length). Accordingly, $N$ is approximately the laser power divided by the mean power in a speckle, $N = P_{\text{L}}/\langle P_{\text{s}}\rangle$. The laser power is the average intensity times the cross-sectional area $\left(P_{\text{L}} = I_0\sigma_b\right)$. To determine the mean power in a speckle, we first average over the probability density of speckle intensities to obtain the mean speckle intensity $\left\langle I/I_0\right\rangle = \int_0^\infty uP(u)\mathrm{d}u$, where $P(u) = -\partial P\left(I/I_0 > u\right)/\partial u$. Equations (3) and (4) give

$$\left\langle I/I_0\right\rangle_{\text{2-D}} = \mu_2 - \left(\mu_2 + u_{\text{s2}}\right)e^{-u_{\text{s2}}/\mu_2} + A_2 e^{-u_{\text{s2}}}\left[4+\pi+(4+\pi)u_{\text{s2}} + (2+\pi)u_{\text{s2}}^2\right]/4, \tag{7}$$

$$\left\langle I/I_0\right\rangle_{\text{3-D}} = \mu_3 - \left(\mu_3 + u_{\text{s3}}\right)e^{-u_{\text{s3}}/\mu_3} + A_3\left[\frac{3\sqrt{\pi}}{5}\operatorname{erfc}\left(\sqrt{u_{\text{s3}}}\right) + e^{-u_{\text{s3}}}\sqrt{u_{\text{s3}}}\left(u_{\text{s3}}^2 + \frac{7}{10}u_{\text{s3}} + \frac{6}{5}\right)\right], \tag{8}$$

where erfc($x$) is the complementary error function. For speckles with a Gaussian transverse profile $\left[I(r) = Ie^{-\left(2\sqrt{\log 2}\, r/w_{\text{s}}\right)^2}\right]$ and full width at half maximum (FWHM) $w_{\text{s}}$, integration over $r$ gives the mean power in a speckle, $\langle P_{\text{s}}\rangle_{\text{2-D}} = \left\langle I/I_0\right\rangle_{\text{2-D}} I_0 w_{\text{s}}\sqrt{\pi/\log 2}$ and $\langle P_{\text{s}}\rangle_{\text{3-D}} = \left\langle I/I_0\right\rangle_{\text{3-D}} I_0 w_{\text{s}}^2\pi/(4\log 2)$. Finally, the expected number of speckles in 2-D and 3-D, respectively, is

$$N = \frac{\sigma_b}{w_{\text{s}}\left\langle I/I_0\right\rangle_{\text{2-D}}}\sqrt{\frac{\log 2}{\pi}}, \tag{9}$$

$$N = \frac{\sigma_b}{w_s^2 \langle I/I_0 \rangle_{3\text{-D}}} \frac{4\log 2}{\pi}. \tag{10}$$

The single-speckle threshold ($I_{\text{thr,speckle}}$) generally depends on the speckle size, plasma conditions, and the instability under consideration. An analytic approximation can be obtained by constructing a spatially localized solution out of the linear eigenmodes for a plane-wave drive laser,[19] but it is not sufficiently accurate for quantitative applications. Here we take a semi-analytic approach where the speckle statistics are given by Eqs. (5) and (6), while $I_{\text{thr,speckle}}$ is taken from single-speckle *LPSE* simulations.

Figure 1 compares Eq. (1) to various speckled-beam *LPSE* calculations. The thresholds are normalized to the threshold for a single plane-wave drive beam, $I_{\text{thr,TPD}}$ (Ref. 19). Figure 1(a) shows 2-D calculations using a single beam with a varying *f* number at $L_n = 200\ \mu$m, $T_e = 2$ keV, and $L_n = 400\ \mu$m, $T_e = 4$ keV, which are similar to the conditions in direct-drive ICF experiments on the OMEGA[20] and National Ignition Facility[15] lasers, respectively. The thresholds are higher in the longer-scale-length calculations because, for a given speckle width, the single-speckle threshold increases with increasing temperature and scale length. The non-monotonic nature of the thresholds is a result of the competition between the increasing thresholds with decreasing speckle size and the increased number of speckles with decreasing *f* number.

Figures 1(b) and 1(c) show 3-D instability thresholds for $L_n = 200\ \mu$m, $T_e = 2$ keV and $L_n = 400\ \mu$m, $T_e = 4$ keV, respectively, for three different beam configurations: (1) a single beam with varying *f* number; (2) six *f*/6.7 beams uniformly distributed on a cone relative to the *x* axis with polar angle $\theta$ and azimuthal angle for the *m*th beam $\varphi_m = 2\pi m/6$; and (3) eight *f*/6.7 beams organized into two four-beam cones with polar angles $\theta$ and $\theta/2$ and azimuthal angles $\varphi_m = 2\pi m/4$ and $\varphi_m = 2\pi m/4 + \pi/4$, respectively. For the multibeam cases, the horizontal axis corresponds to an effective *f* number given by the cone angle, $f_\# = 1/(2\tan\theta)$ and the beam polarizations were aligned. All three beam configurations give the same threshold to within statistical variations and are in good agreement with the semi-analytic model. This shows that the instability behavior is predominantly determined by the smallest (and highest intensity) speckles and justifies the treatment of the cones of beams as a single beam with a small effective *f* number.

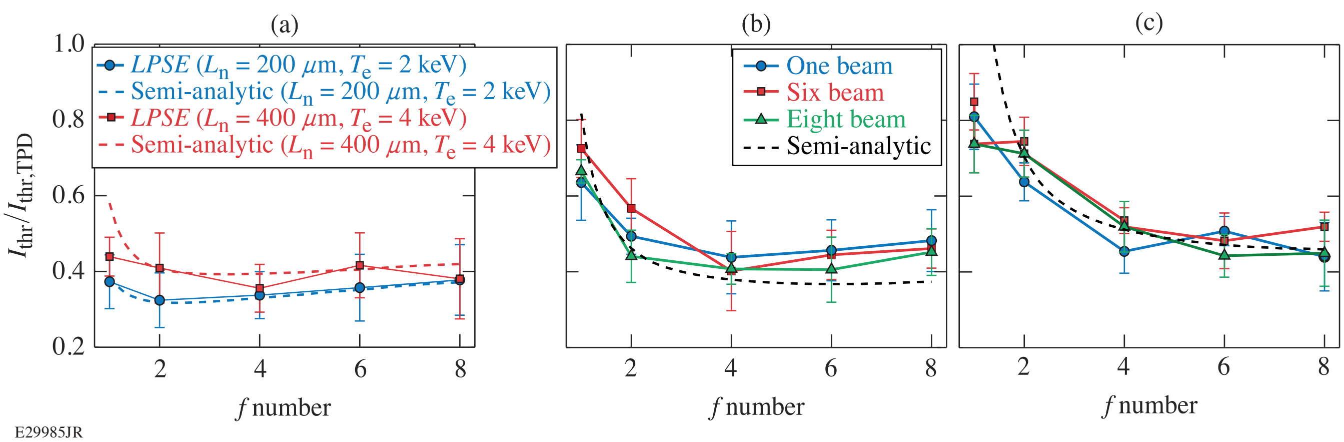


Figure 1
Absolute TPD instability thresholds for speckled beams (normalized to the plane-wave threshold). (a) Two-dimensional *LPSE* calculations at $L_n = 200\ \mu$m, $T_e$ = 2 keV (blue circles), and $L_n = 400\ \mu$m, $T_e = 4$ keV (red squares). [(b),(c)] Three-dimensional *LPSE* calculations show $L_n = 200\ \mu$m, $T_e = 2$ keV and $L_n = 400\ \mu$m, $T_e = 4$ keV, respectively, for one beam (blue circles), six beams (red squares), and eight beams (green triangles). The dashed curves show the corresponding semi-analytic results. The error bars correspond to the standard deviation from an ensemble of 20 (5) speckle realizations in 2-D (3-D).

This material is based upon work supported by the Department of Energy National Nuclear Security Administration under Award Number DE-NA0003856, ARPA-E BETHE grant number DE-FOA-0002212, the University of Rochester, and the New York State Energy Research and Development Authority.

1. S. Atzeni and J. Meyer-ter-Vehn, *The Physics of Inertial Fusion: Beam Plasma Interaction, Hydrodynamics, Hot Dense Matter*, 1st ed., International Series of Monographs on Physics, Vol. 125 (Oxford University Press, Oxford, 2004).
2. W. L. Kruer, *The Physics of Laser Plasma Interactions, Frontiers in Physics*, Vol. 73, edited by D. Pines (Addison-Wesley, Redwood City, CA, 1988).
3. R. S. Craxton *et al*., Phys. Plasmas **22**, 110501 (2015).
4. Y. Kato *et al*., Phys. Rev. Lett. **53**, 1057 (1984).
5. C. Stoeckl *et al*., Phys. Rev. Lett. **90**, 235002 (2003).
6. H. A. Rose and D. F. DuBois, Phys. Rev. Lett. **72**, 2883 (1994).
7. V. T. Tikhonchuk, C. Labaune, and H. A. Baldis, Phys. Plasmas **3**, 3777 (1996).
8. D. F. DuBois, B. Bezzerides, and H. A. Rose, Phys. Fluids B **4**, 241 (1992).
9. D. T. Michel *et al*., Phys. Rev. Lett. **109**, 155007 (2012).
10. P. Michel *et al*., Phys. Rev. Lett. **115**, 055003 (2015).
11. J. Zhang *et al*., Phys. Rev. Lett. **113**, 105001 (2014).
12. D. T. Michel *et al*., Phys. Plasmas **20**, 055703 (2013).
13. J. F. Myatt *et al*., Phys. Plasmas **21**, 055501 (2014).
14. R. K. Follett *et al*., Phys. Plasmas **24**, 102134 (2017).
15. M. J. Rosenberg *et al*., Phys. Rev. Lett. **120**, 055001 (2018).
16. R. K. Follett *et al*., Phys. Rev. E **101**, 043214 (2020).
17. B. Eisenberg, Stat. Probab. Lett. **78**, 135 (2008).
18. J. Garnier, Phys. Plasmas **6**, 1601 (1999).
19. A. Simon *et al*., Phys. Fluids **26**, 3107 (1983).
20. T. R. Boehly *et al*., J. Appl. Phys. **85**, 3444 (1999).